The Crystallographic, Spectroscopic and Theoretical Studies on (*E*)-2-[((4-fluorophenyl)imino)methyl]-4-nitrophenol and (*E*)-2-[((3-fluorophenyl)imino)methyl]-4-nitrophenol Compounds

Demirtaş, Güneş**+; Dege, Necmi
Department of Physics, Faculty of Arts and Sciences, Ondokuz Mayıs University, 55139 Samsun, TURKEY

Ağar, Erbil; Şahin, Songül
Department of Chemistry, Faculty of Arts and Sciences, Ondokuz Mayıs University, 55139 Samsun, TURKEY

ABSTRACT: *In this study, two new salicylideneaniline derivative compounds which are an isomer of each other have been synthesized and characterized by X-Ray Diffraction (XRD) technique, IR spectroscopy, and theoretical method. While (E)-4-(dihydroxyamino)-2-(((4-fluorophenyl)imino) methyl)phenol (**1**), crystalizes triclinic P-1 space group, (E)-4-(dihydroxyamino)-2-(((3-fluorophenyl)imino)methyl)phenol (**2**) crystalizes monoclinic $P2_1/c$ space group. Both of the molecules which adopt (E) configuration with respect to the central C=N bond have strong intermolecular O—H···N hydrogen bonds. These O—H···N hydrogen bonds create S(6) motifs according to graph set notation. The optimized geometries of the molecules have been calculated by using Density Functional Theory (DFT) with the 6-31G(d,p) basis set. Molecular Electrostatic Potential (MEP) map and Frontier Molecular Orbitals have been made for the optimized geometries. In addition to these studies, the theoretical IR spectra of the compounds, the experimental IR spectra of which have been recorded at 4000-400 cm^{-1} interval, have also been calculated with same level theory. The experimental and theoretical results were compared to each other.*

KEYWORDS: *Salicylideneaniline; Isomer; Tautomerism; DFT; IR.*

INTRODUCTION

The molecules which contain C═N double bond are expressed as Schiff base. Schiff bases are generated by the reaction between primary amine and aldehyde. Schiff base compounds may display photochromic, thermochromic and solvatochromic properties [1-4]. Salicylideneanilines which are Schiff base compounds exhibit these properties in the solid state, too [2, 3]. Therefore, salicylideneanilines and its complexes are used in many fields of chemistry and biochemistry. Furthermore, salicylideneanilines are also used at technologic areas such as the control and measurement of radiation intensity, optical computers and display systems [5-7]. These compounds have intramolecular O—H···N or N—H···O hydrogen bonds and these hydrogen bonds create a double minimum potential well [8].

** To whom correspondence should be addressed.*
+ E-mail: gunesd@omu.edu.tr
1021-9986/2018/5/55-65 11/$/5.01

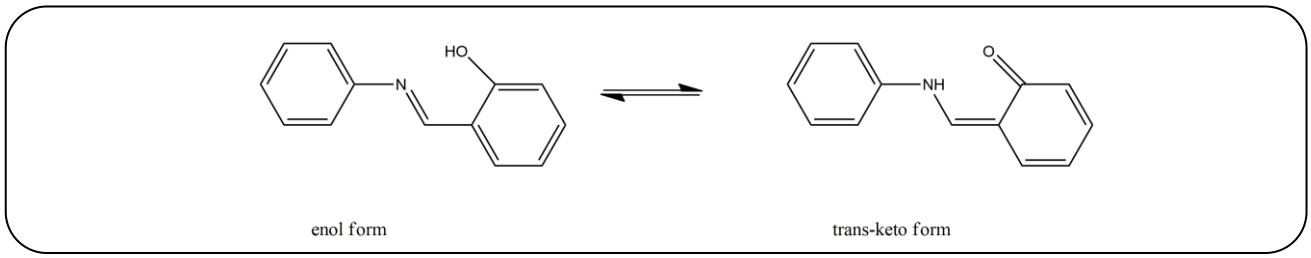

Scheme 1: Enol and keto tautomeric forms of salicylideneaniline.

Therefore Excited State Intramolecular Proton Transfer (ESIPT) studies for salicylideneaniline derivatives are interested [9-12]. Additionally, salicylideneaniline derivative compounds display tautomerism. These compounds exhibit in two tautomeric forms as enol and keto forms in the solid state. Tautomerism occurs by intermolecular proton transfer from the oxygen atom to the nitrogen atom. In thermochromic salicydeneanilines, the enol form is more stable than the cis-keto form [13]. Therefore, photochromic salicylideneaniline derivatives usually exist enol form and have a yellow color in the crystal state. When these compounds are exposed to UV-light, the proton bonded to hydroxyl oxygen moves from hydroxyl oxygen to imine nitrogen. The photoproduct which occurs with the rearrangement of the molecule's geometry is red color [14-16]. Such a proton transfer changes π-electron system of the molecule [17, 18]. Tautomerism for salicylideneaniline can be seen in Scheme 1.

In this study, crystallographic, theoretical and spectroscopic studies of (*E*)-4-(dihydroxyamino)-2-(((4-fluorophenyl)imino)methyl)phenol and (*E*)-4-(dihydroxyamino)-2-(((3-fluorophenyl)imino)methyl)phenol which are salicylideneaniline derivative compounds have been investigated.

EXPERIMENTAL SECTION

Synthesis

The (*E*)-2-[((4-fluorophenyl)imino)methyl]-4-nitrophenol compound was prepared by reflux a mixture of a solution containing 2-hydroxy-5-nitrobenzaldehyde (0.157 g, 1.0 mmol) in 20 mL ethanol and a solution containing 4-fluoroaniline (0.010 g, 1.0 mmol) in 20 mL ethanol. The reaction mixture was stirred for 4 h under reflux. The suitable crystals of (*E*)-2-[((4-fluorophenyl)imino)methyl]-4-nitrophenol for X-ray analysis were obtained from ethyl alcohol by slow evaporation.

The (*E*)-2-[((3-fluorophenyl)imino)methyl]-4-nitrophenol compound was prepared by reflux a mixture of a solution containing 2-hydroxy-5-nitrobenzaldehyde (0.157 g, 1.0 mmol) in 20 mL ethanol and a solution containing 3-fluoroaniline (0.010 g, 1.0 mmol) in 20 mL ethanol. The reaction mixture was stirred for 4 h under reflux. The suitable crystals of (*E*)-2-[((3-fluorophenyl)imino)methyl]-4-nitrophenol for X-ray analysis were obtained from ethyl alcohol by slow evaporation.

Spectroscopy

The IR spectra of the compounds as a KBr pellet were recorded from 4000 to 400 cm^{-1} with a Bruker Vertex 80 V FT-IR spectrometer.

Computational Methods

Geometrical parameters of the compounds and harmonic vibrational frequencies were calculated using the Gaussian 03 program package [19] and DFT/B3LYP approach in conjunction with the 6-31G(d,p) basis set. The vibrational frequencies were scaled by 0.9611 for DFT B3LYP/6-31G(d,p) [20]. The theoretical spectra of the compounds were made using the Gauss-View molecular visualization program [21]. For modeling, the values obtained from the X-ray coordinates were used as the initial values.

X-Ray Crystallography

Single-crystal X-ray data were collected on a Stoe IPDS II [22] single crystal diffractometer using monochromatic MoK_α radiation at 296 K. X-AREA [22] and X-RED [22] programs were used to cell refinement and data reduction, respectively. SHELXS-97 [23] and SHELXL-97 [23] programs were used to solve and refine the structures, respectively. ORTEP-3 for Windows [24] was used to prepare the figures. WinGX [25] and PLATON [26] software were used to prepare material for publication.

H atoms of hydroxyl groups were located difference maps and were refined isotropically. The O—H distances are 0.90 (4) Å for compound **1**, 0.94 (5) Å for compound **2**. Other hydrogen atoms were positioned geometrically (C—H=0.930 Å) and treated as riding with U_{iso}(H)=1.2U_{eq}(C). Non-hydrogen atoms were located difference map and the crystal structure was refined anisotropically. In the compound **2**, DELU restrains in SHELXL-97 were applied to minimize the component of the anisotropic displacement parameters of atoms along with their chemical bonds for C8—C9 and C3—F1.

The crystal data and refinement of the compounds are shown in Table 1.

RESULTS AND DISCUSS

Crystallographic Studies

(*E*)-2-[((4-fluorophenyl)imino)methyl]-4-nitrophenol, compound **1**, and (*E*)-2-[((3-fluorophenyl)imino)methyl]-4-nitrophenol, compound **2**, are salicylideneaniline derivative compounds and these compounds are an isomer of each other. While compound **1** contains fluorine atom in para-position, compound **2** contains fluorine atom in meta-position.

Both of the compounds have two aromatic rings and these aromatic rings are almost planar (RMSE values of C1/C6 and C8/C13 rings are 0.0082 Å, 0.0013 Å for compound **1**; 0.0022 Å, 0.0052 Å for compound **2**, respectively). Dihedral angles between these aromatic rings are 37.36 (7)° for compound **1**, 31.33 (13)° for compound **2**.

The C7═N1, C9—O1 and C7—C8 bond distances are 1.276 (3) Å, 1.336 (3) Å and 1.463 (4) Å for compound **1**; 1.289 (5) Å, 1.330 (5) Å and 1.448 (6) Å for compound **2**, respectively. Because of these bond distances, it can be said that the molecules crystalize enol-imine tautomeric form. Additionally, both of the compounds adopt (*E*) configuration with respect to the central C═N bond. Some crystal structures which have the same conformation have been reported in the literature [27-32]. The O2—N2—O3 bond angles and C8—C7═N1—C1 torsion angles are 122.5 (2)°, 180.0 (3)° for compound **1**; 122.5 (4)°, −178.7 (4)° for compound **2**, respectively. The C—C aromatic bond distances range from 1.353 (4) Å to 1.416 (3) Å for molecule **1**, from 1.348 (8) Å to 1.407 (6) Å for molecule **2**.

As can be seen in Figs. 1a and 1b, the compounds have strong intramolecular O—H···N hydrogen bonds. These intramolecular hydrogen bonds create S(6) motifs with respect to graph set notation. In addition to these O—H···N hydrogen bonds, while the crystal structure of the compound **1** has C—H···O, C—H···F and weak π···π interactions, the crystal structure of the compound **2** has C—H···O hydrogen bond and weak π···π interactions. While intermolecular C7—H7···O3 hydrogen bonds in the compounds create $R_2^2(14)$ motifs according to graph set notation, intermolecular C4—H4···O2 hydrogen bonds in the compound 2 create C(12) motifs along the b-axis. The geometric parameters of these hydrogen bonds are given in Table 2. The crystal packing of the compounds created *via* these intermolecular interactions can be seen in Fig. 2. The X-ray data show that the N2—O2 and N2—O3 bond distances are 1.217 (3) Å and 1.233 (3) Å for compound **1**; 1.228 (5) Å and 1.229 (5) Å for compound **2**, respectively. Because of intermolecular hydrogen bonds, the N2—O3 bond distance for compound **1** is longer than the N2—O2 bond distance. The N—O bond distances of the compound **2** are almost similar level.

Theoretical Studies

For compound **1**, the RMSE value between the bond distances which were obtained by XRD technique and the bond distances which were calculated by DFT method is 0.0179 Å. This value for compound **2** is 0.0190 Å. For bond angles of compound **1**, the RMSE between experimental and theoretical values was calculated as 0.8459°. For compound **2**, the RMSE value is 1.1619° for experimental and DFT method.

For compound **1,** the C1—N1—C7—C8 torsion angle which is obtained by X-ray diffraction technique is 180.0 (3)°, this torsion angle was calculated as −177.5823° by DFT method. These values of compound **2** are −178.7 (4)° and −177.8088°, respectively. The dihedral angles between aromatic rings were detected 37.36 (7)° for compound **1**, 31.33 (13)° for compound **2** by XRD. The dihedral angles calculated by DFT method are 31.86° for compound **1** and 32.93° for compound **2**. Some selected theoretical and experimental bond distances, bond angles and torsion angles of the compounds can be seen in Table 3.

Theoretical values calculated by DFT method are close to the experimental values. Therefore these theoretical geometries of the molecules overlap with the experimental geometries.

Table 1: Results of refinement parameters and diffraction X-ray data for compounds 1, 2.

	Compound (1)	Compound (2)
Formula	$C_{13}H_9FN_2O_3$	$C_{13}H_9FN_2O_3$
Crystal system	Triclinic	Monoclinic
Color / Shape	Yellow / Plate	Yellow / Prism
Crystal size	0.41×0.20×0.01 mm	0.72×0.31×0.02 mm
Temperature	296 K	296 K
Space group	P-1	$P2_1/c$
Unit cell dimensions		
a	3.7753 (6) Å	3.7636 (4) Å
b	12.5132 (19) Å	24.314 (4) Å
c	13.005 (2) Å	13.0454 (15) Å
α	79.146 (12)°	90°
β	81.911 (12)°	97.663 (9)°
γ	88.881 (12)°	90°
h / k / l	-4, 4 / -15, 15 / -16, 16	-4, 4 / -30, 30 / -16, 16
Volume	597.36 (16) $Å^3$	1183.1 (3) $Å^3$
Z	2	4
Density (calculated)	1.447 mg/m^3	1.461 mg/m^3
Radiation	MoKα (λ=0.71073 Å)	MoKα (λ=0.71073 Å)
Reflections collected	7108	11042
Absorption coefficient (μ)	0.12 mm^{-1}	0.12 mm^{-1}
Absorption correction	Integration X-RED	Integration X-RED
F(000)	268	536
θ ranges	12.5-26.5°	1.7-26.5°
Observed reflections, I>2σ(I)	1316	807
Independent reflections	2453 (Rint=0.062)	2465 (Rint=0.151)
Measured reflections	7108	11042
Data / Restrains / Parameters	2453 / 0 / 176	2465 / 2 / 176
Maximum shift / error	0.00	0.00
Goodness-of-fit on F^2	1.01	0.95
Final R indices [I>2σ(I)]	R1=0.058, $wR(F^2)$=0.101	R1=0.076, $wR(F^2)$=0.196
Largest diff. Peak and hole	−0.15 $eÅ^3$ 0.13 $eÅ^3$	−0.17 $eÅ^3$ 0.16 $eÅ^3$

Table 2: Hydrogen bond geometries of the compounds (Å, °).

D—H···*A*	*D*—H	H···*A*	*D*···*A*	*D*—H···*A*
Compound (1)				
O1—H1*O*···N1	0.90 (4)	1.77 (4)	2.594 (3)	151 (3)
C7—H7···O3^{i}	0.93	2.56	3.400 (3)	151
C11—H11···F1^{ii}	0.93	2.55	3.205 (3)	128
Compound (2)				
O1—H1*O*···N1	0.92 (5)	1.79 (5)	2.598 (6)	146 (4)
C4—H4···O2^{i}	0.93	2.59	3.457 (7)	156
C7—H7···O3^{ii}	0.93	2.57	3.396 (6)	149

Symmetry codes for compound (1): (i) −x+1, −y+1/2, −z+1, (ii) x−1, y+1, z; Symmetry codes for compound (2): (i) −x+1, y+1/2, −z+3/2; (ii) −x+1, −y+1, −z+1.

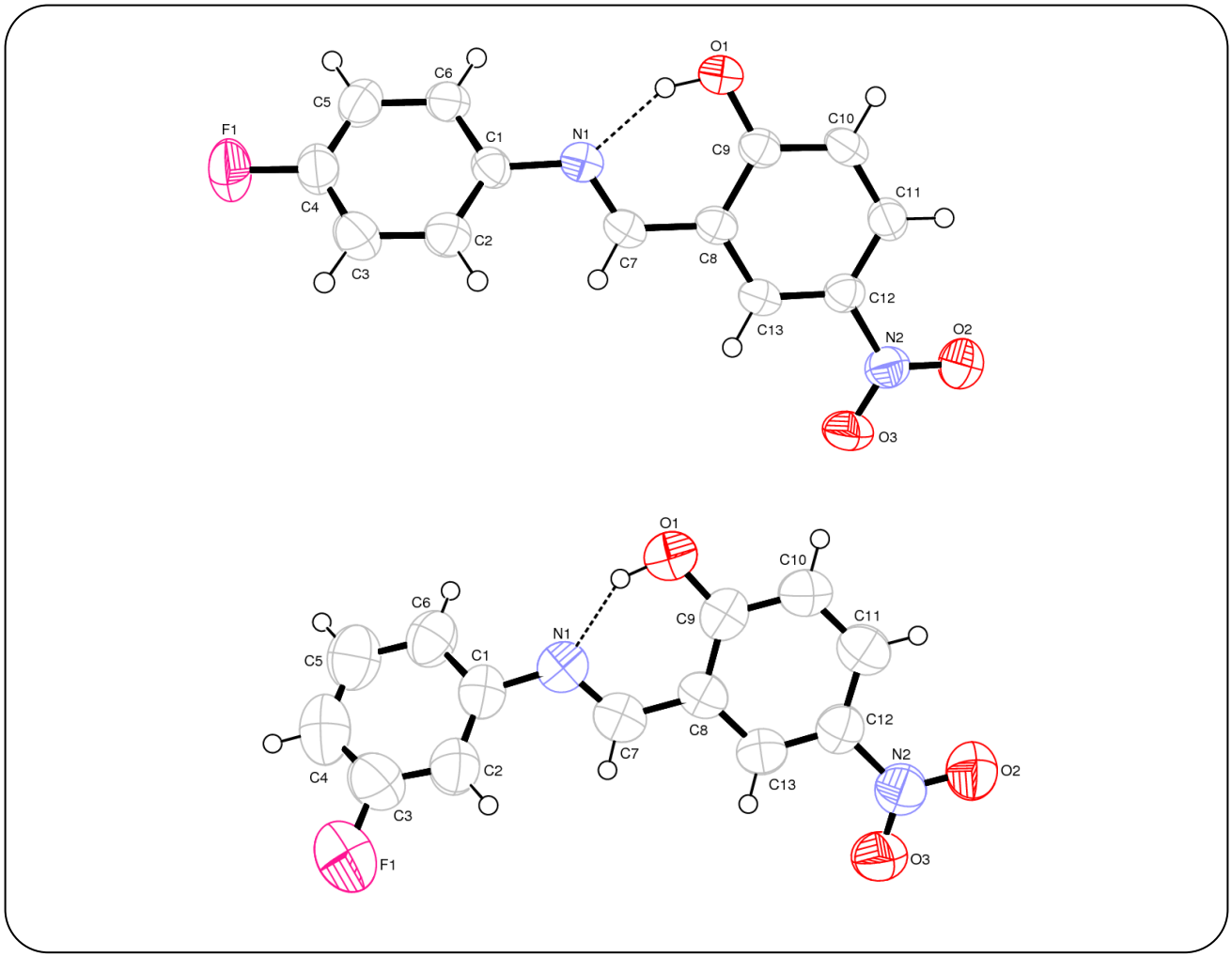

Fig. 1: a) The molecular structure of compound 1, with the atom-numbering scheme. Displacement ellipsoids are drawn at the 50% probability level. The intramolecular hydrogen bond is shown by dashed lines. b) The molecular structure of compound 2, with the atom-numbering scheme. Displacement ellipsoids are drawn at the 50% probability level. The intramolecular hydrogen bond is shown by dashed lines.

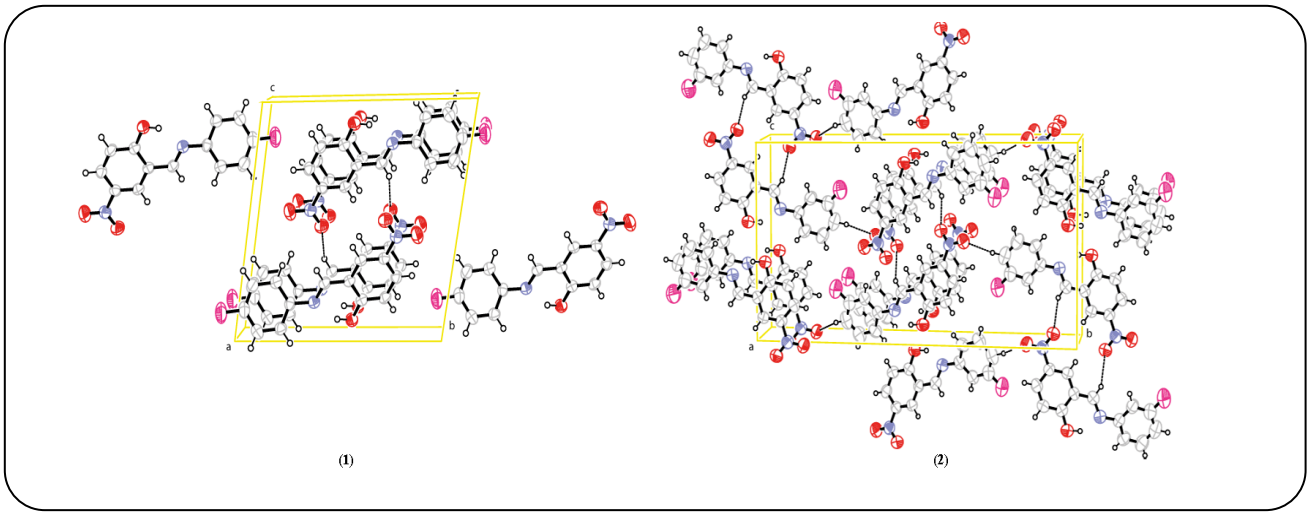

Fig. 1: Packing diagram of the title compounds with the intermolecular C—H···O hydrogen bonds. Hydrogen bonds are drawn with dashed lines.

Frontier molecular orbitals

LUMO+1, LUMO, HOMO and HOMO-1 orbitals obtained by DFT method of the molecules are seen in Figs. 3a and 3b. If the frontier molecular orbitals obtained by DFT method of the compound **1** are considered, the distributions of LUMO, HOMO, and HOMO-1 orbitals can be seen on all surface of the molecule. In LUMO+1, molecular orbitals concentrate on nitrophenol. In compound **2**, the distributions of molecular orbitals are very similar to compound **1**. While the molecular orbitals in LUMO, HOMO, and HOMO-1 distribute on all surface of the molecule, the molecular orbitals in LUMO+1 distribute on 4-nitrophenol. HOMO-LUMO gap energies are 4.1002 eV for compound **1**, 4.1579 eV for compound **2**. These high values for HOMO-LUMO gap energies show that the molecules have chemical stability.

Molecular Electrostatic Potential (MEP) maps

We used the values of MEP that correspond to surface as determined from points with electronic density ρ=0.0004 a.u. The Molecular Electrostatic Potential (MEP) maps which were calculated by DFT method for molecules are shown in Fig. 4. If the MEP of molecule **1** is considered, electrophilic attach centers can be seen at the vicinity of oxygen atoms. In addition to these regions, the environment of the fluorine atom has a negative charge density. From X-ray data, the intermolecular interactions were detected at the vicinity of oxygen atoms and the fluorine atom that act at weak intermolecular interactions. The charge densities of some regions of compound **1** are almost −0.0489 a.u. for the region between O2 and O3 atoms, −0.0121 a.u. for the environment of a fluorine atom and −0.0250 a.u. for the environment of O1 atom.

For compound **2**, the molecular electrostatic potential map is similar to compound **1**'s MEP. The most negative regions are at the vicinity of oxygen atoms and a fluorine atom. The *V(r)* values of these regions are −0.0247 a.u. for O1 atom, −0.0486 a.u. for the region between O2 and O3 atoms and −0.0127 a.u. for fluorine atom.

IR Studies

The experimental and theoretical IR spectra of compound **1** are seen in Fig. 5a. According to the experimental spectrum, the absorption band at 1624 cm^{-1} is attributed to the υ(C═N) stretching vibration of the compound **1**. The theoretical stretching vibrations belong to this bond are calculated at 1620.66 cm^{-1} for DFT. The υ(C—O) stretching vibration values of compound **1** are at 1294 cm^{-1} for experimentally, 1297.8 cm^{-1} for DFT. The experimental υ(O—H) vibrations can be seen at 3724 cm^{-1} as a broaden curve, because of the strong intramolecular hydrogen bond.

The experimental and theoretical IR spectra of compound **2** are given in Fig. 5b. For compound **2**, while the absorption band at about 1626 cm^{-1} is attributed to υ(C═N) stretching vibration, theoretical values of this

Table 3: Some selected experimental and theoretical structural parameters of the title compounds (Å, °).

	Compound (1)		Compound (2)	
Atoms	X-Ray	DFT	X-Ray	DFT
C1—N1	1.432 (3)	1.4087	1.419 (6)	1.4086
C3—F1	-	-	1.379 (7)	1.3484
C4—F1	1.369 (3)	1.3472	-	-
C7—C8	1.463 (4)	1.4525	1.448 (6)	1.4518
C7—N1	1.276 (3)	1.2913	1.289 (5)	1.2914
C9—O1	1.336 (3)	1.3303	1.330 (5)	1.3300
C12—N2	1.461 (3)	1.4605	1.462 (6)	1.4608
N2—O2	1.217 (3)	1.2325	1.229 (5)	1.2324
N2—O3	1.233 (3)	1.2333	1.228 (5)	1.2331
C2—C1—N1	122.9 (2)	123.4346	122.9 (5)	122.8113
C6—C1—N1	116.8 (2)	117.4384	116.8 (5)	117.5408
C2—C3—F1	-	-	117.6 (7)	118.4366
C4—C3—F1	-	-	117.0 (7)	118.9320
C3—C4—F1	118.3 (3)	118.9920	-	-
C5—C4—F1	118.2 (3)	119.0750	-	-
N1—C7—C8	121.3 (3)	121.5704	122.5 (5)	121.5420
C7—C8—C9	120.7 (2)	121.0255	120.1 (5)	121.0089
C7—C8—C13	119.9 (3)	119.8890	120.4 (5)	119.8704
O1—C9—C8	122.0 (2)	121.6242	122.8 (5)	121.6759
O1—C9—C10	118.7 (3)	118.7495	117.7 (5)	118.7220
C11—C12—N2	119.4 (2)	119.4456	118.7 (5)	119.4227
C13—C12—N2	119.0 (2)	119.2163	118.7 (5)	119.2340
C1—N1—C7	119.8 (2)	121.8807	120.8 (4)	121.7329
O2—N2—C12	118.8 (3)	117.7291	118.7 (5)	117.7033
O3—N2—C12	118.7 (2)	117.8090	118.8 (4)	117.8016
O2—N2—O3	122.5 (2)	124.4619	122.5 (4)	124.4950
N1—C7—C8—C9	−1.0 (4)	0.0990	−2.5 (7)	0.1392
C7—C8—C9—O1	1.7 (4)	−0.0930	2.0 (7)	−0.0697
C6—C1—N1—C7	−143.8 (2)	−150.7504	−147.5 (5)	−149.4595
C8—C7—N1—C1	180.0 (3)	−177.5823	−178.7 (4)	−177.8088
C11—C12—N2—O2	2.9 (4)	−0.2522	7.8 (6)	−0.1970

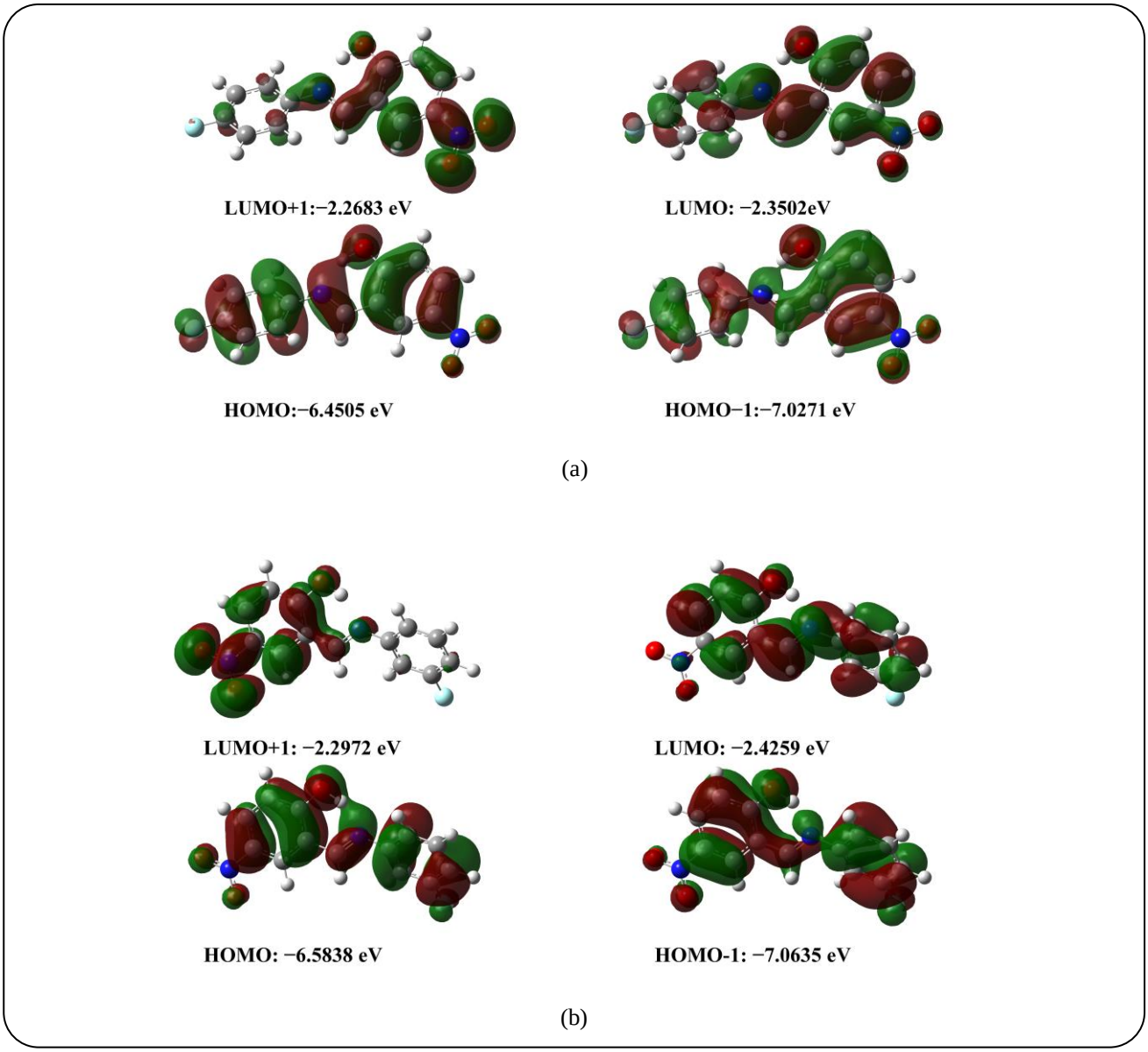

Fig. 3: (a) Molecular orbital surfaces and energy levels are given for HOMO-1, HOMO, LUMO and LUMO+1 of the compound 1 computed by DFT at the B3LYP/6-31G (d,p). (b) Molecular orbital surfaces and energy levels are given for HOMO-1, HOMO, LUMO and LUMO+1 of the compound 2 computed by DFT at the B3LYP/6-31G (d,p).

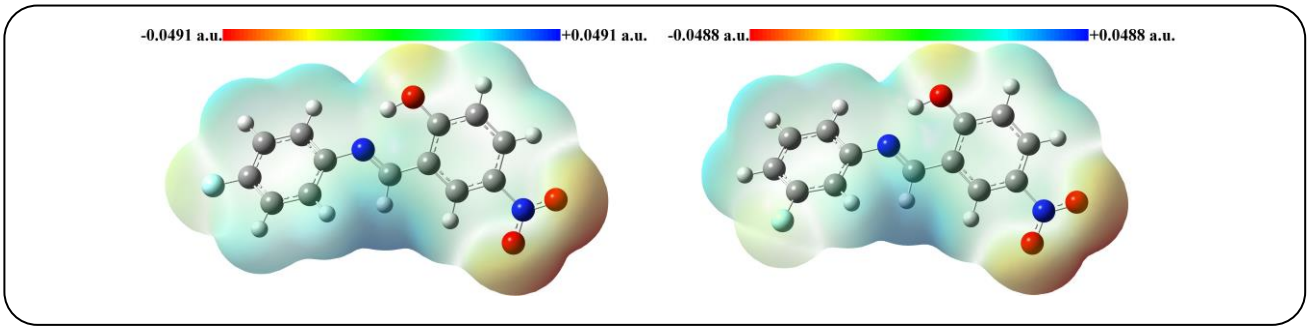

Fig. 4: Molecular electrostatic potential map of the compounds calculated by DFT at the B3LYP/6-31G (d, p).

Table 4: Some experimental and theoretical vibration frequencies of the compounds (cm^{-1}).

	Compound (1)		Compound (2)	
Vibration Bands	Experimental	DFT	Experimental	DFT
ν(O—H)	3724	2961.37, 2944.15	3452	2963.97, 2947.42
ν(C—O)	1294	1297.80	1298	1295.73
ν(C═N)	1624	1620.66	1626	1620.98
ν(C—H) Aromatic	3100, 3070	3119.04-3076.56	3095-3059	3119.51-3074.79
ν(C—C) Aromatic	1570, 1590	1617.96, 1591.08	1591, 1573	1618.95, 1587.73

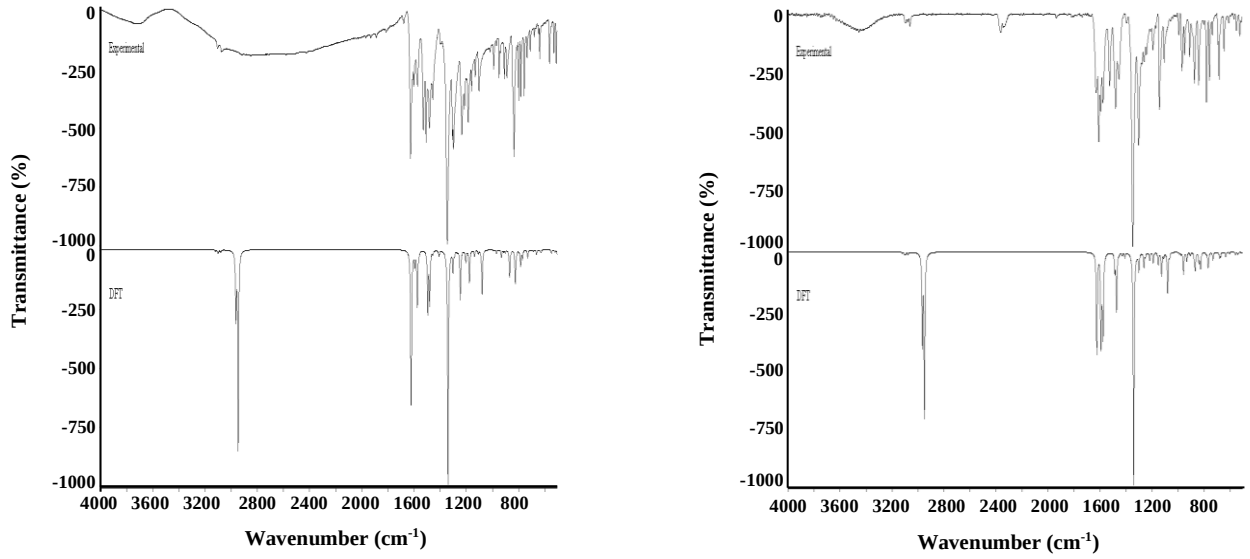

Fig. 5: (a) Experimental and theoretical IR spectra of the compound 1 in 4000–500 cm^{-1} region. (b) The experimental and theoretical IR spectrum of the compound 2 in 4000–500 cm^{-1} region.

vibration are at 1620.98 cm^{-1} for DFT. The υ(C—O) band was observed experimentally at 1298 cm^{-1}. The theoretical values of this stretching vibration are at 1295.73 cm^{-1} for DFT. The υ(O—H) stretching vibration was recorded at 3452 cm^{-1} like a broaden curve, due to the intramolecular hydrogen bond. These stretching vibrations are consistent with the literature [32-35]. Some stretching vibrations of compound **1** and compound **2** are given in Table 4.

CONCLUSIONS

In this paper, the crystal structures of two new molecules which are an isomer of each other were determined. The fluorine atoms are bonded para- and meta-position to molecules and this modification changes the crystal structure of the molecules. The crystallographic data show that the molecules have strong intermolecular hydrogen bonds.

The distributions of the frontier molecular orbitals are similar both of molecules. Because of large HOMO-LUMO gap energy, the molecules have chemical stability.

According to MEP, the electrophilic attach centers of the molecules are at the vicinity of oxygen atoms and a fluorine atom. The crystallographic results show that these regions have intermolecular interactions.

Due to intermolecular hydrogen bonds, the ν(O—H) stretching vibrations of molecules are detected as broadening curves and these results agree with the crystallographic studies.

Appendix A. Supplementary Data

CCDC 951327 (**1**) and CCDC 951320 (**2**) contain the supplementary crystallographic data for this paper. This data can be obtained free of charge via https://www.ccdc.cam.ac.uk/services/structure_deposit/ or from the Cambridge Crystallographic Data Centre, 12 Union Road, Cambridge CB2 1EZ, UK; fax: (+44) 1223 336 033; or e-mail: deposit@ccdc.cam.ac.uk.

Acknowledgement

The authors thank Ondokuz Mayıs University Research Fund for financial support of this study (Project No: PYO.FEN.1904.09.006).

Received : Apr. 20, 2016 ; Accepted : Nov. 20, 2017

REFERENCES

[1] Hadjoudis E., Vittorakis M., Moustakali-Mavridis I., Photochromism and Thermochromism of Schiff Bases in the Solid State and in Rigid Glasses, *Tetrahedron*, **43**: 1345-1360 (1987).

[2] Ohshima A., Momotake A., Arai T., Photochromism, Thermochromism, and Solvatochromism of Naphthalene-Based Analogues of Salicylideneaniline in Solution, *J. Photoch. Photobio.* A, **162**: 473-479 (2004).

[3] Cohen M. D., Schmidt G. M. J., Photochromy and Termochromy of Anils[1], *J. Phys. Chem.*, **66**: 2442-2446 (1962).

[4] Bouas-Laurent H., Dürr H., Organic Photochromism, *Pure Appl. Chem.*, **73**:639-665 (2001).

[5] Elmali A., Elerman Y., Zeyrek C. T., Conformational Sudy and Structure of N-(2,5-methylphenyl) Salicylaldimine, *J. Mol. Struct.*, **443**: 123-130 (1998).

[6] Brown G.H., "Photochromism, Techniques of Chemistry", Vol. III, Wiley-Interscience, New York (1971).

[7] Dürr H., Bouas-Laurent H., "Photochromism: Molecules and Systems, Elsevier", Amsterdam (1990).

[8] Tayyari S. F., Zeegers-Huyskens Th., Wood J. L., Spectroscopic Study of Hydrogen Bonding in the Enol form of β-diketones—II. Symmetry of the Hydrogen Bond, *Spectrochim. Acta A* **35**:1289-1295 (1979).

[9] Ogawa K., Harada J., Fujiwara T., Yoshida S., Thermochromism of Salicylideneanilines in Solution: Aggregation-controlled Proton Tautomerization, *J. Phys. Chem. A* **105**: 3425-3427 (2001).

[10] Ameer-Beg S., Ormson S.M., Brown R.G., Matousek P., Towrie M., Nibbering E.T.J., Foggi P., Neuwahl F. V. R., Ultrafast Measurements of Excited State Intramolecular Proton Transfer (ESIPT) in Room Temperature Solutions of 3-Hydroxyflavone and Derivatives, *J. Phys. Chem. A* **105**: 3709-3718 (2001).

[11] Sliwa M., Mouton N., Ruckebusch C., Aloïse S., Poizat O., Buntinx G., Métivier R., Nakatani K., Masuhara H., Asahi T., Comparative Investigation of Ultrafast Photoinduced Processes in Salicylidene-Aminopyridine in Solution and Solid State, *J. Phys. Chem., C* **113**: 11959-11968 (2009).

[12] Becker R. S., Lenoble C., Zein A., Photophysics and Photochemistry of the Nitro Derivatives of Salicylideneaniline and 2-(2'-Hydroxyphenyl)benzothiazole and Solvent Effects, *J. Phys. Chem.*, **91**: 3517- (1987).

[13] Harada J., Fujiwara T., Ogawa K., Crucial Role of Fluorescence in the Solid-State Thermochromism of Salicylideneanilines, *J. Am. Chem. Soc.*, **129**: 16216-16221 (2007).

[14] Harada J., Uekusa H., Ohashi Y., X-ray Analysis of Structural Changes in Photochromic Salicylideneaniline Crystals. Solid-State Reaction Induced by Two-Photon Excitation, *J. Am. Chem. Soc.*, **121**: 5809-5810 (1999).

[15] Destro R., Gavezzotti A., Simonetta M., Salicylideneaniline, *Acta Cryst.*, **B34**: 2867-2869 (1978).

[16] Isse A. A., Abdurrahman A. M., Vianello E., Role of Proton Transfer in the Electrochemical Reduction Mechanism of Salicylideneaniline, *J. Electroanal. Chem.*, **431**: 249-255 (1997).

[17] Ito E., Oji H., Araki T., Oichi K., Ishii H., Ouchi Y., Ohta T., Kosugi N., Maruyama Y., Naito T., Inabe T., Seki K., Soft X-ray Absorption and X-ray Photoelectron Spectroscopic Study of Tautomerism in Intramolecular Hydrogen Bonds of N-Salicylideneaniline Derivatives, *J. Am. Chem. Soc.*, **119**: 6336-6344 (1997).

[18] Sekikawa T., Kobayashi T., Inabe T., Femtosecond Fluorescence Study of the Substitution Effect on the Proton Transfer in Thermochromic Salicylideneaniline Crystals, *J. Phys. Chem. A*, **101**:644-649 (1997).

[19] Frisch M. J., Trucks G. W., Schlegel H. B., Scuseria G. E., Robb M. A., Cheeseman J. R., Montgomery J. A., Jr, Vreven T., Kudin K. N., Burant J. C., Millam J. M., Iyengar S. S., Tomasi J., Barone V., Mennucci B., Cossi M., Scalmani G., Rega N., Petersson G. A., Nakatsuji H., Hada M., Ehara M., Toyota K., Fukuda R., Hasegawa J., Ishida M., Nakajima T., Honda Y., Kitao O., Nakai H., Klene M., Li X., Knox J. E., Hratchian H. P., Cross J. B., Adamo C., Jaramillo J., Gomperts R., Stratmann R. E., Yazyev O., Austin A. J., Cammi R., Pomelli C., Ochterski J. W., Ayala P. Y., Morokuma K., Voth G. A., Salvador P., Dannenberg J. J., Zakrzewski V. G., Dapprich S., Daniels A. D., Strain M. C., Farkas O., Malick D. K., Rabuck A. D., Raghavachari K., Foresman J. B., Ortiz J. V., Cui Q., Baboul A. G., Clifford S., Cioslowski J., Stefanov B. B., Liu G., Liashenko A., Piskorz P., Komaromi I., Martin R. L., Fox D. J., Keith T., Al-Laham M. A., Peng C. Y., Nanayakkara A., Challacombe M., Gill P. M. W., Johnson B., Chen W., Wong M. W., Gonzalez C., Pople J. A., Gaussian 03, Revision E.01., Gaussian, Inc., Pittsburgh (2004).

[20] Irikura K. K., Johnson III R. D., Kacker R. N., Uncertainties in Scaling Factors for ab Initio Vibrational Frequencies, *J. Phys. Chem., A* **109**: 8430-8437 (2005).

[21] Frisch A., Dennington II R., Keith T., Millam J., Nielsen A. B., Holder A. J., Hiscocks J., GaussView Reference Version 40, Gaussian Inc., Pittsburgh (2007).

[22] Stoe & Cie, X-AREA (Version 1.18) and Stoe & Cie, X-RED32 (Version 1.04), Darmstadt, Germany (2002).

[23] Sheldrick G. M., A Short History of SHELX, *Acta Crystallogr.*, **A64**: 112-122 (2008).

[24] Farrugia L. J., ORTEP-3 for Windows-A Version of ORTEP-III with a Graphical User Interface (GUI), *J. Appl. Cryst.*, **30**: 565-565 (1997).

[25] Farrugia L.J., WinGX Suite for Small-Molecule Single-Crystal Crystallography, *J. Appl. Cryst.*, **32**: 837-838 (1999).

[26] Spek A. L., Single-Crystal Structure Validation with the Program PLATON, *J. Appl. Cryst.*, **36**:7-13 (2003).

[27] Alaman Ağar A., Tanak H., Yavuz M., Experimental and Quantum Chemical Calculational studies on 2-[(4-propylphenylimino)methyl]-4-nitrophenol, *Mol. Phys.*, **108**: 1759-1772 (2010).

[28] Kılıç I., Ağar E., Erşahin F., Işık Ş., 2-[(4-Methoxyphenyl)iminomethyl]-4-nitrophenol, *Acta Crystallogr.*, **E65**: o737 (2009).

[29] Valkonen A., Kolehmainen E., Grzegórska A., Ośmiałowski B., Gawinecki R., Rissanen K., Two (E)-2-({[4-(dialkylamino)phenyl]-imino}methyl)-4-Nitrophenols, *Acta Crystallogr.*, **C68**: o279-o282 (2012).

[30] Tan Y.-H., Teoh S. G., Loh W.-S., Fun H.-K., 4- [(2-Hydroxy-5-nitrobenzylidene)-amino] benzenesulfonamide, *Acta Crystallogr.*, **E66**: o2610-o2611 (2010).

[31] Özdemir Tarı G., Ceylan U., Macit M., Isık Ş., (E)-2-[(4-Iodophenyl)iminomethyl]-6-methylphenol, *Acta Crystallogr.*, **E66**:o1568 (2010).

[32] Demirtaş G., Dege N., Ağar E., Gümüş Uzun S., The Crystallographic, Spectroscopic and Theoretical Studies on (E)-2-(((4-chlorophenyl)imino)methyl)-5-(diethylamino)phenol and (E)-2-(((3-chlorophenyl)imino)methyl)-5-(diethylamino)phenol Molecules, *J. Mol. Struct.*, 1152:199-206 (2018).

[33] Albayrak Ç., Frank R., Spectroscopic, Molecular Structure Characterizations and Quantum Chemical Computational Studies of (E)-5-(diethylamino)-2-[(2-fluorophenylimino)methyl]phenol, *J. Mol. Struct.*, **984**: 214-220 (2010).

[34] Albayrak Ç., Kaştaş G., Odabaşoğlu M., Frank R., Survey of Conformational Isomerism in (E)-2-[(4-bromophenylimino)methyl]-5- (diethylamino)phenol Compound from Structural and Thermochemical Points of View, *Spectrochim. Acta A*, **95**: 664-669 (2012).

[35] Kaştaş G., Albayrak Ç., Odabaşoğlu M., Frank R., Single Stranded Helical Chains of C—H···π Interactions Further Connected by Halogen–Halogen Interactions of Type I to Construct Supramolecular Structure of (E)-5-(diethylamino)-2-[(4-iodophenylimino)methyl]phenol Compound, *Spectrochim. Acta A*, **94** :200-204 (2012).